National Renewable Energy Laboratory
Innovation for Our Energy Future

Device Physics of Nanoscale Interdigitated Solar Cells

Wyatt Metzger and Dean Levi

National Renewable Energy Laboratory • Golden, CO 80401

DEVICE MODELS: 2 cases of interdigitated cells

Standard 1D solar cell

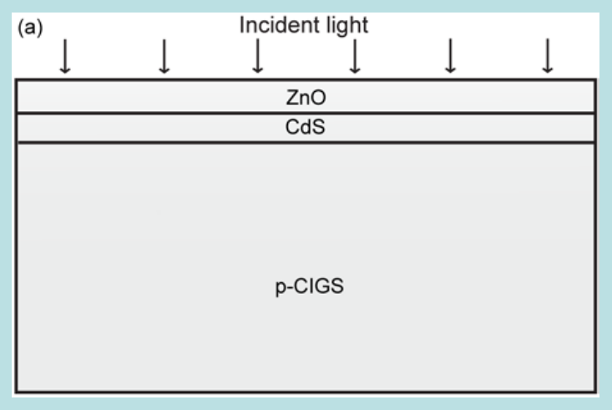

Case 1: No band offsets

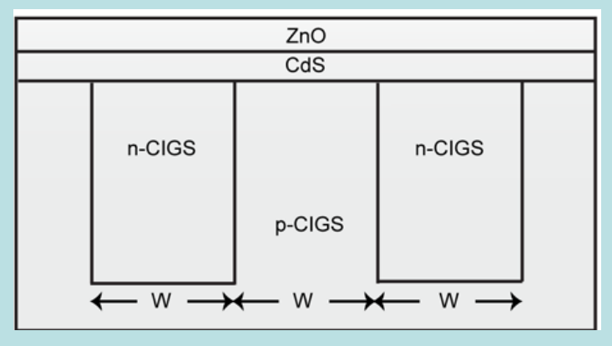

- No band offsets between *p*- and *n*-type regions
- α-phase CIGS absorber
- emitter = 50 nm *n*-CdS and 200 nm ZnO

Common Elements to both cases

- 3 mm thick CIGS absorber layer
- Interdigitated *p*- and *n*- regions of equal width W; 10 nm < W < 1 mm
- *n*-type regions extend 2.5 mm into absorber
- *n*-type doping constant at 6×10^{17} cm^{-3}
- *p*-type doping varied from 6×10^{17} cm^{-3} to 1.2×10^{18} cm^{-3}
- Device performance calculated for 'high quality' and 'low quality' CIGS absorber

Case 2: Varied band offsets

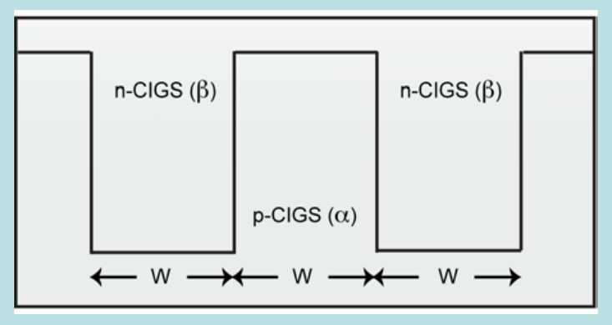

- offsets between *p*- and *n*-type regions varied
- Interdigitated α-like and β-like phase CIGS
- emitter = 50 nm *n*-CdS

MOTIVATION

- Nanoscale interdigitated solar cell device architectures are being investigated for organic and inorganic solar cell devices.
- Due to the inherent complexity of these device designs quantitative modeling is needed to understand the device physics.
- Theoretical concepts have been proposed that nanodomains of different phases may form in polycrystalline CIGS solar cells.
- These theories propose that the nanodomains may form complex 3D intertwined *p-n* networks that enhance device performance.
- Recent experimental evidence offers some support for the existence of nanodomains in CIGS thin films.
- This study utilizes CIGS solar cells to examine general and CIGS-specific concepts in nanoscale interdigitated solar cells.

Material Parameters

Bulk Properties	ZnO	CdS	α-CIGS	β-CIGS
E_g (eV)	3.3	2.4	1.15	1.43
χ (eV)	4.6	4.6	4.6	4.62
μ_e (cm^2/V-s)	100	100	100/10	100/10
μ_h (cm^2/V-s)	25	25	12.5/1.25	12.5/1.25
n, *p* (cm^{-3})	n: 10^{18}	n: 6.0×10^{17}	varied	varied
$\varepsilon/\varepsilon_0$	9	10	13.6	13.6
m_e/m_o	0.2	0.2	0.09	0.09
m_h/m_o	1.2	0.8	0.72	0.72
Midgap state (cm^{-3})	N_a: 10^{16}	N_a: 10^{16}	N_o: 1×10^{15}	N_o: 1×10^{15}
σ_e (cm^2)	10^{-16}	10^{-15}	$2\times10^{-14/-13}$	$2\times10^{-14/-13}$
σ_h (cm^2)	10^{-13}	10^{-12}	$2\times10^{-14/-13}$	$2\times10^{-14/-13}$
Surface Properties	Front	Back		
S_e (cm/s)	10^7	10^7		
S_h (cm/s)	10^7	10^7		
Reflectivity	0.05	0		

COMPUTATIONAL APPROACH

- Device performance was calculated by solving the Poisson and electron-hole continuity equations using the drift-diffusion model and by solving current and energy density boundary equations at heterointerfaces described by the Anderson model.
- Programming was done within the Sentaurus Device simulation environment.

CASE 1: n and p regions both α-phase CIGS
p-doping varies, W varies
$E_g(n) = E_g(p) = 1.15$ eV
n = 6x1017 cm-3
p = 6.0x1017, 6.2x1017 cm-3

Band bending vs W for equal doping
$n = p = 6\times10^{17}$ cm^{-3}

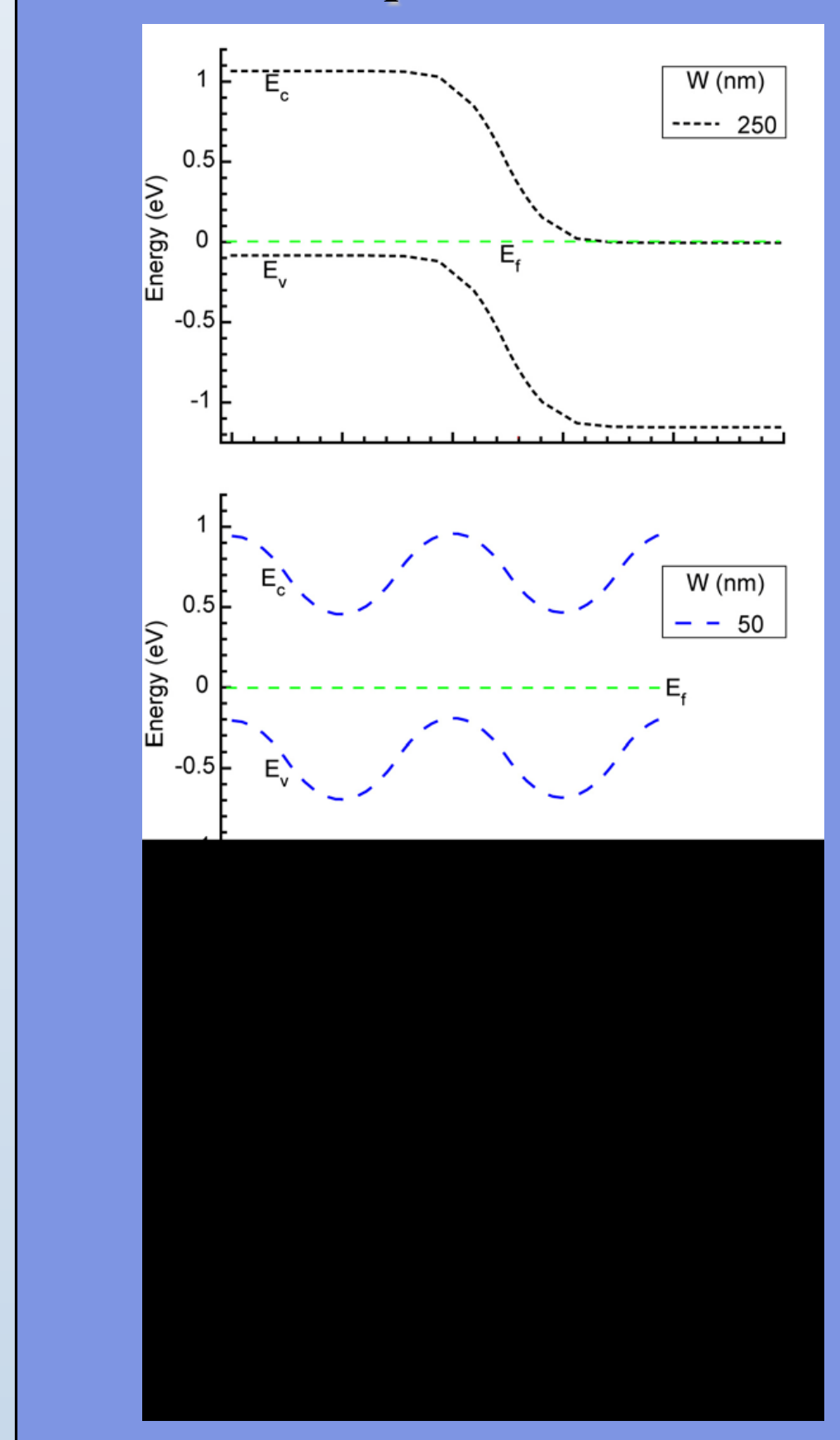

As W decreases less charge is available to create band bending, the built-in field at the vertical *p-n* junction decreases, and the device becomes a 1D solar cell with average properties of the *n* and *p* regions.

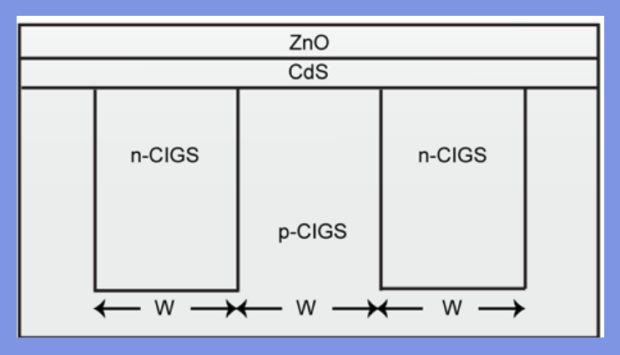

Current flow pathways

W = 50 nm

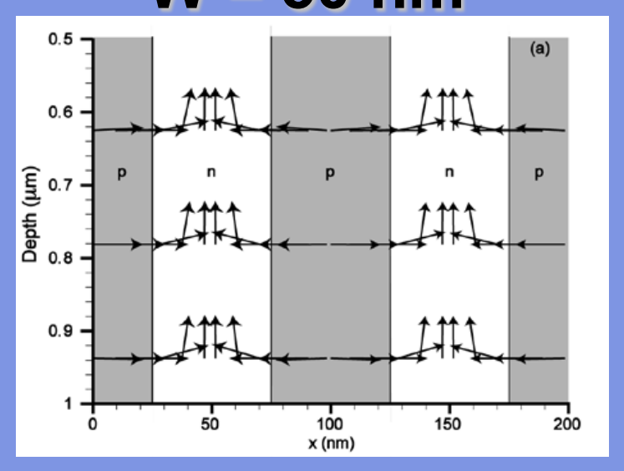

W = 10 nm

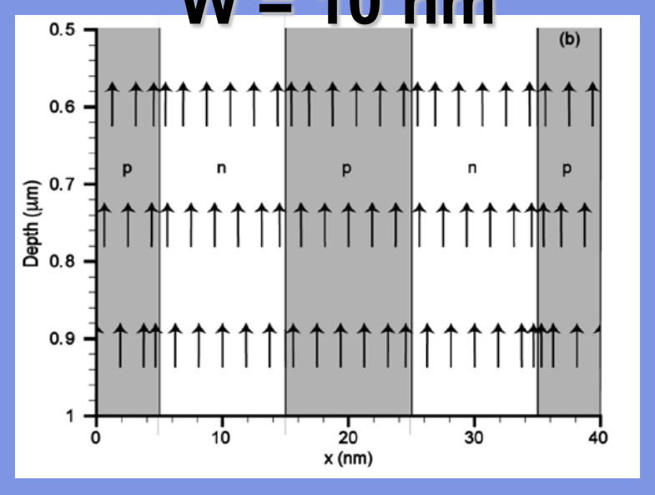

Band bending vs W for unequal doping
$n = 6\times10^{17}$ cm^{-3} $p = 6.2\times10^{17}$ cm^{-3}

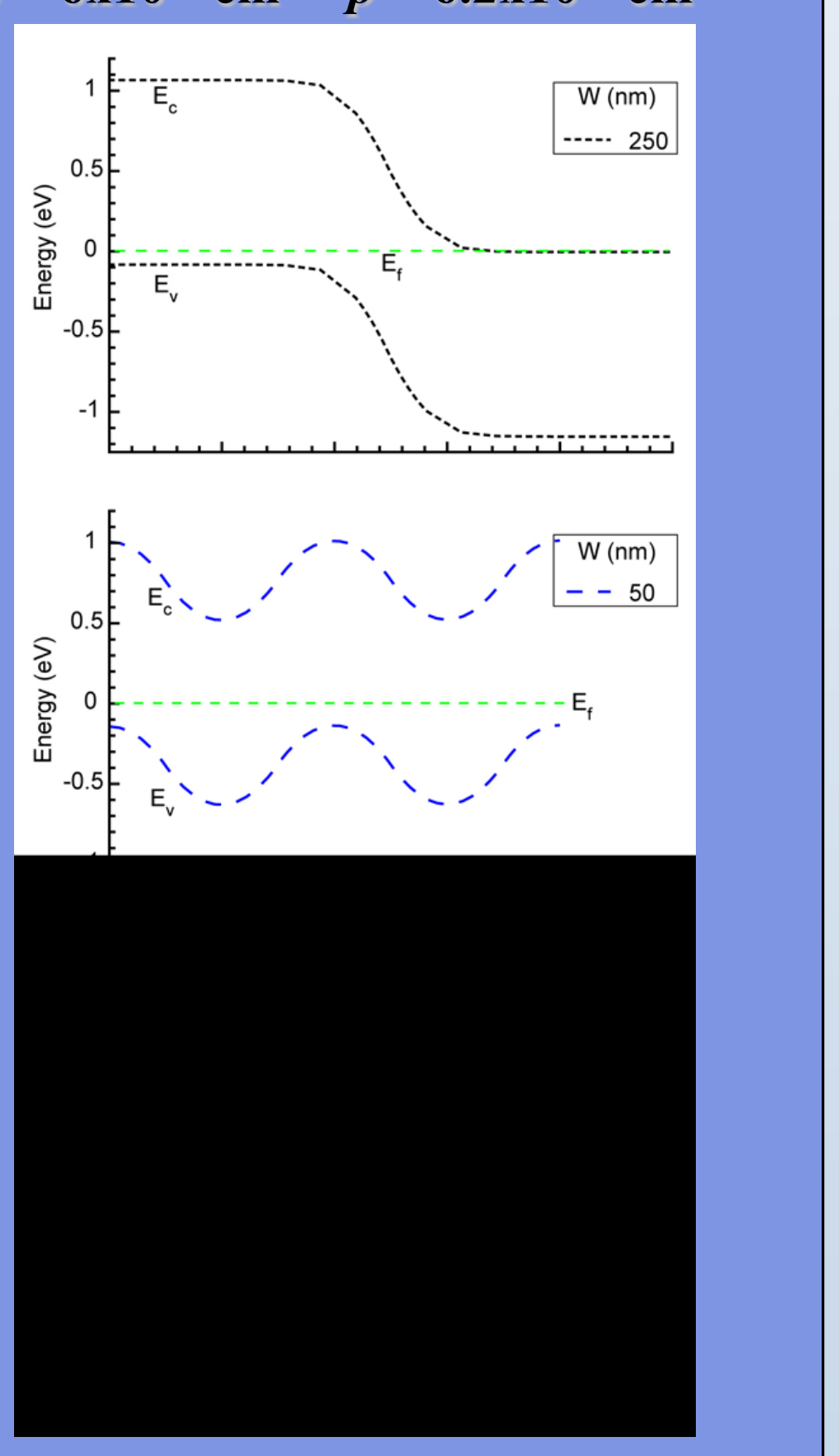

As W decreases less charge is available to create band bending, the built-in field at the vertical *p-n* junction decreases, and the device becomes a 1D solar cell with average properties of the *n* and *p* regions.

"Low quality CIGS"

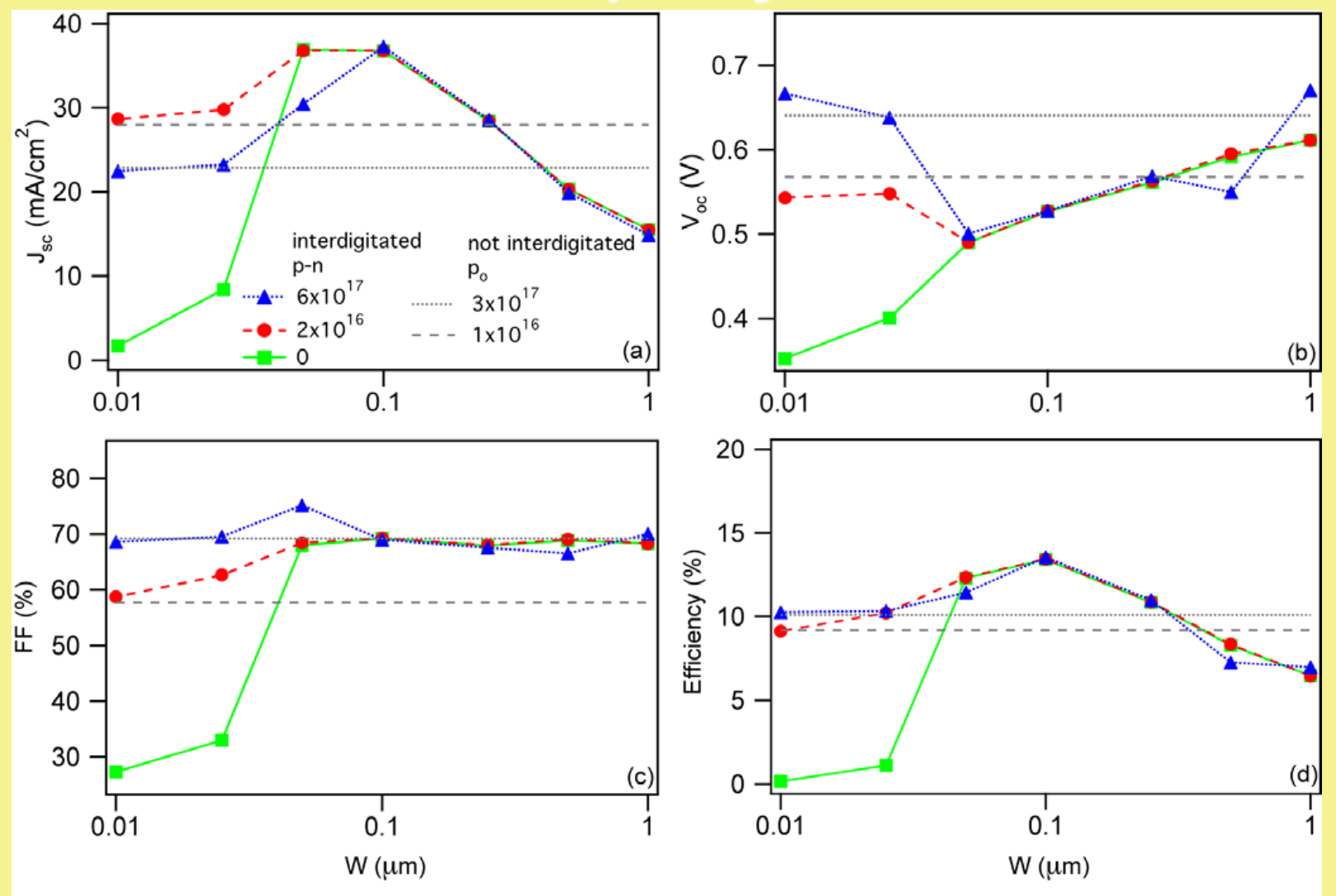

"High quality CIGS"

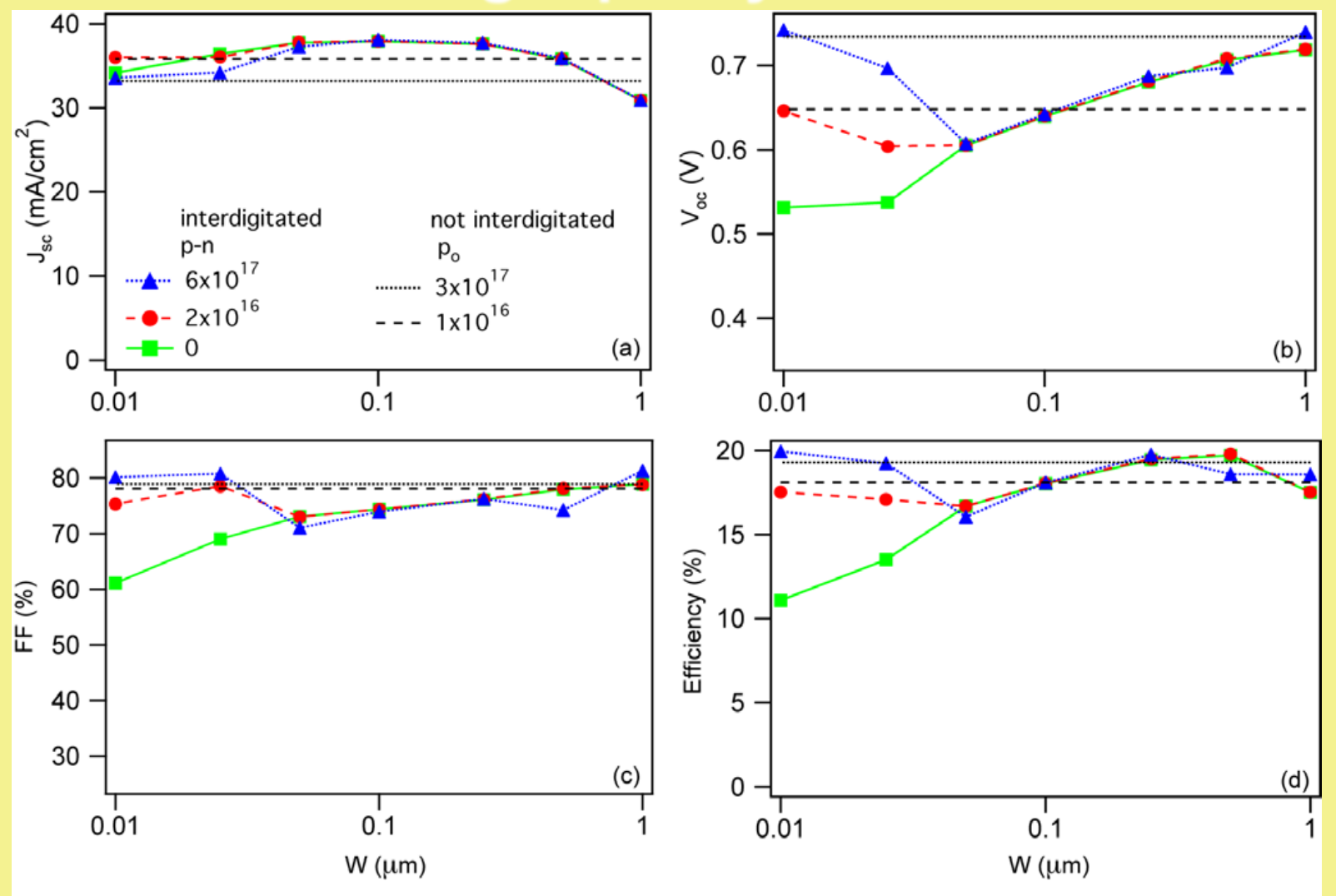

W = 1 um V_{oc} is optimum when there is maximal band bending and minimal dark current, which occurs at large W. But the geometry is not ideal for current collection and J_{sc} is inferior to a comparable planar junction device.

W -> 50 nm As W decreases towards 50 nm, current is collected more efficiently, but increasing dark current and reduced band bending lower V_{oc}. PV designs that increase photocurrent collection generlly increase dark current too.

W < 50 nm The strength of the lateral fields diminish and no longer effectively separate charge. Transport and performance becomes identical to a planar junction device with a uniform doping equivalent to half of *p* – *n* in the CIGS layer.

CASE 2: *n* regions α-phase, *p* regions β-phase
Band offset varies, W varies
$\Delta\chi = -0.3, 0.0, 0.3$ eV
$E_g(\alpha) = 1.15$ eV $E_g(\beta) = 1.45$ eV

Band bending when Dc = 0
n= *p* = 6×10^{17} cm^{-3}

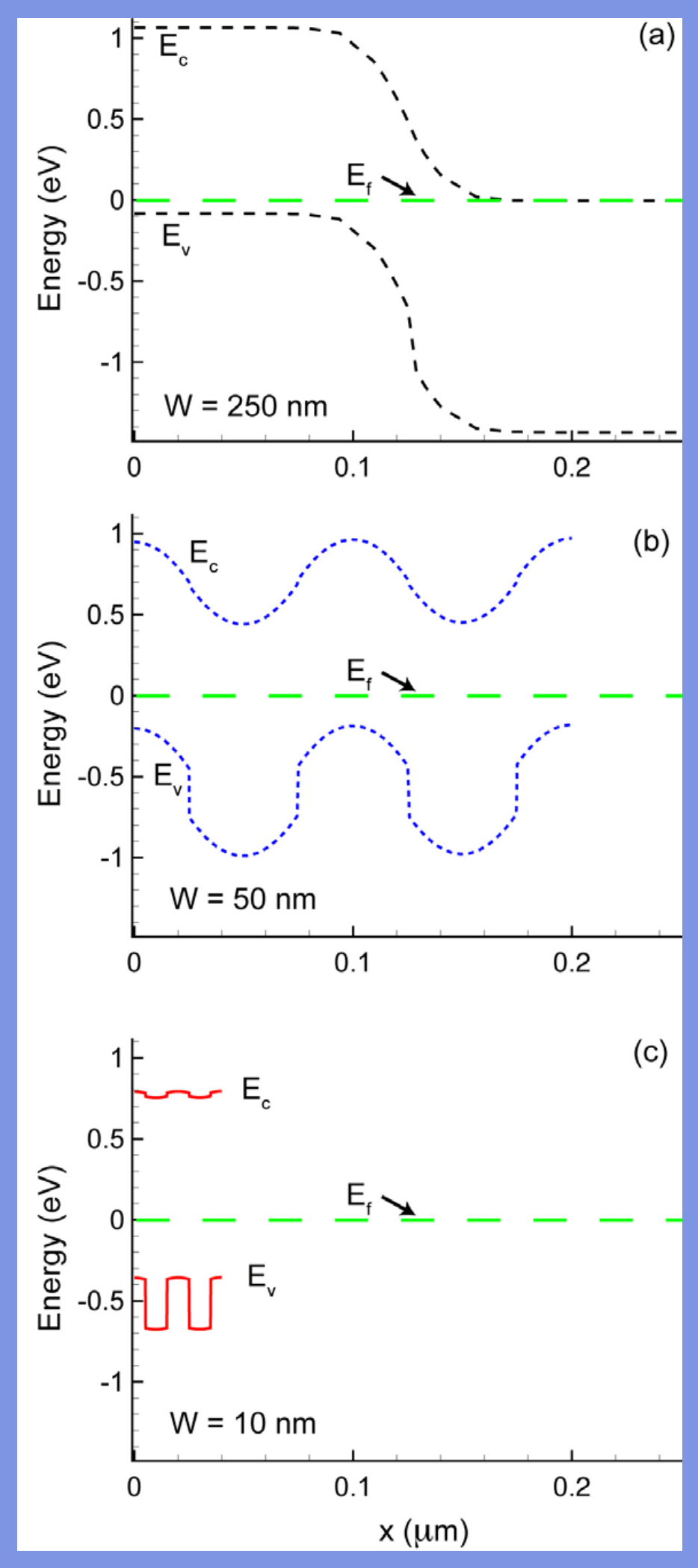

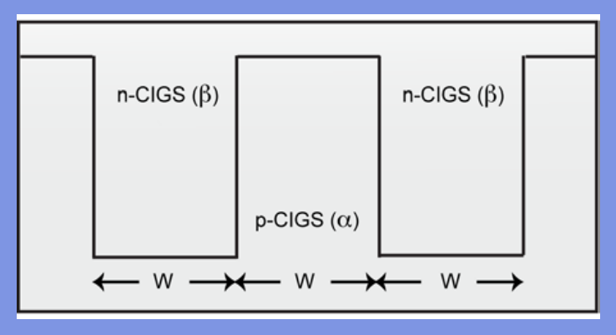

For large W (e.g. 250 nm), the lateral band alignment is determined by charge transfer and band bending (upper left figure).

For intermediate W (e.g. 50 nm), the lateral band alignment is determined both by band bending and band offsets (middle left figure).

For small W (e.g. 10 nm), the lateral band alignment is determined by the bandgap and conduction and valence band offsets and not by band bending (bottom left figure).

If the bandgap and offsets form a robust type II interface (e.g. Δc = -0.3, middle and upper right), charge separation occurs even when W = 10 nm (lower right).

$\Delta\chi$=-0.3 eV
Type II band alignment
Effective carrier localization
Enhanced device performance

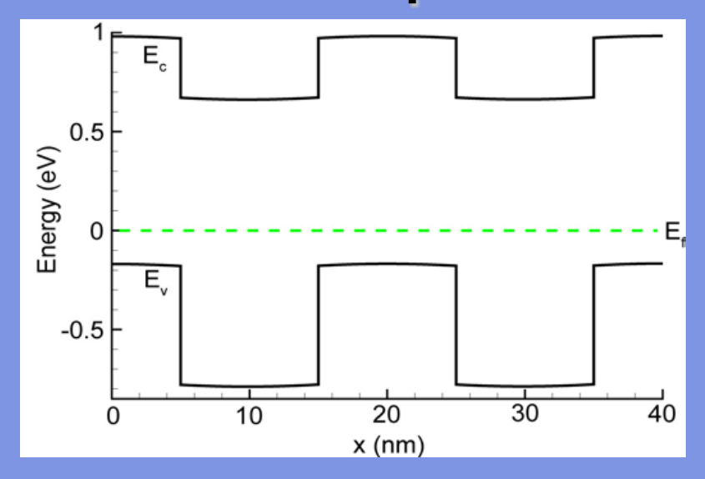

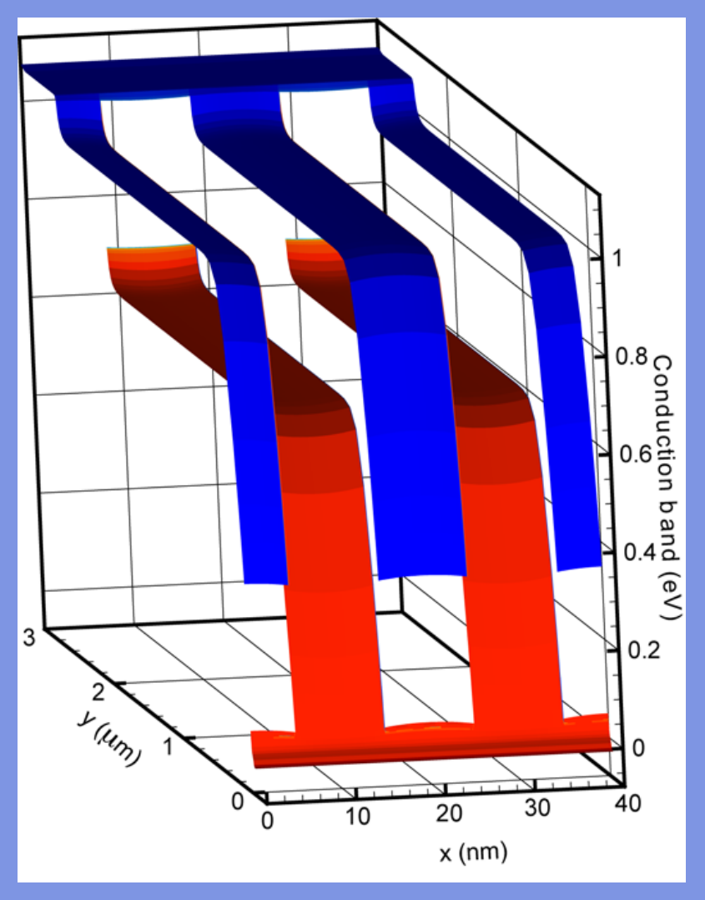

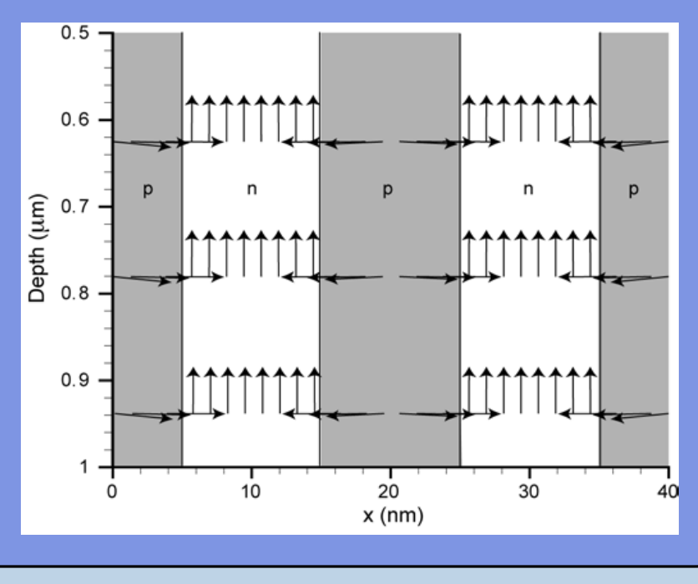

"Low quality CIGS"

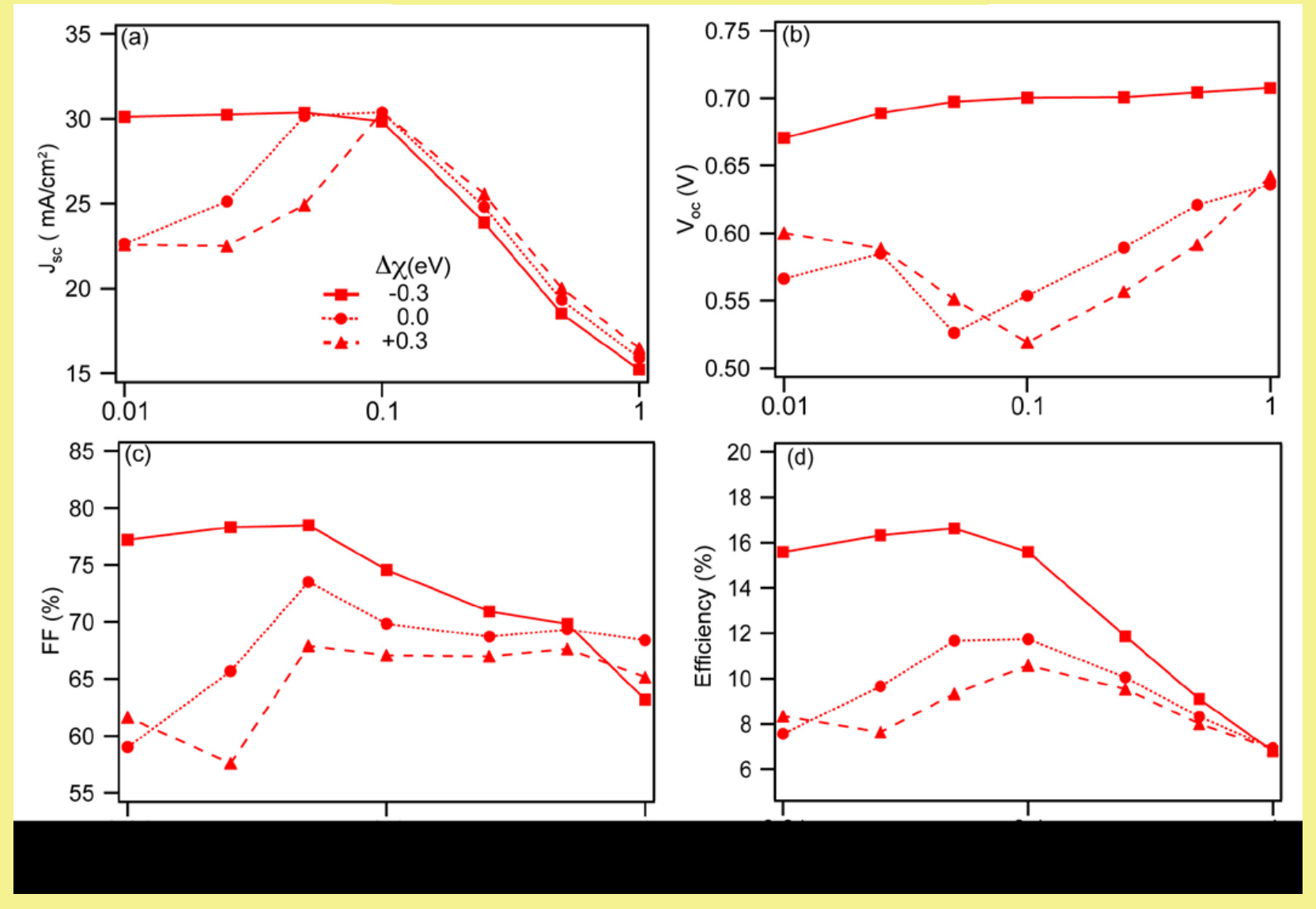

"High quality CIGS"

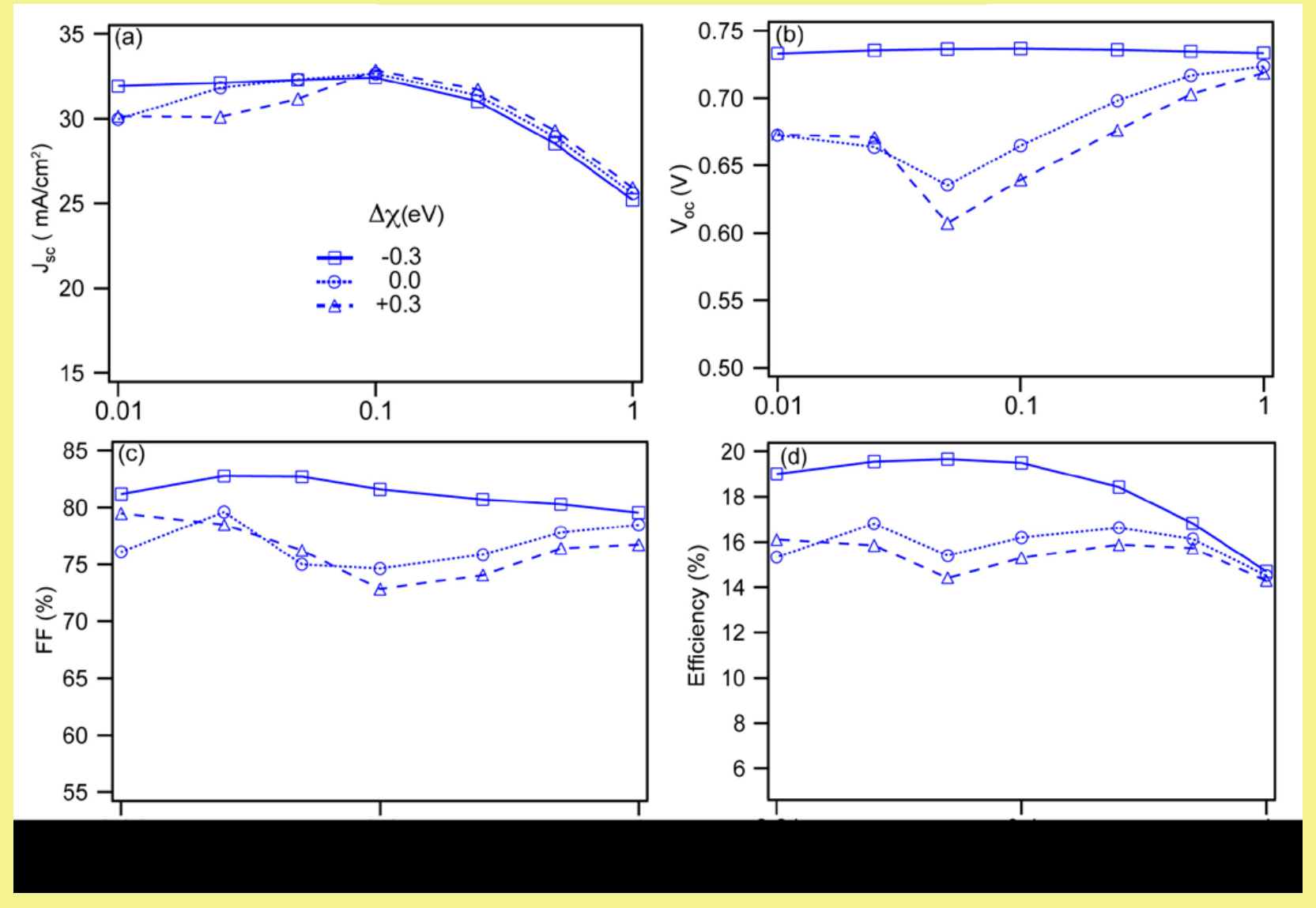

$\Delta\chi$ = 0.0 or +0.3 For W greater than 50 nm, the lateral fields and device performance are similar to the case with no offsets. For W less than 50 nm, either the valence or conduction band is flat. Hence one carrier is not separated laterally and recombination is not effectively reduced,. The results are again similar to the case with no offsets.

$\Delta\chi$ = -0.3 For large W, the lateral fields and device performance are similar to the case with no offsets. However as W is reduced, the offsets form a robust type II junction which effectively separates charge and reduces recombination even for W = 10 nm. This structure improves device performance relative to a planar junction device, and atttains efficiencies greater than 15% even for "low quality" material with a diffusion length of 100 nm.

CONCLUSIONS

- Interdigitated thin-film solar cells can give good device performance commensurate with comparable planar junction devices.
- Interdigitated *p* and *n* regions increase efficiency relative to a comparable planar junction device for low-quality material when W is about 50 or 100 nm in this study.
- In most cases, device performance is generally not significantly increased relative to a planar junction.
- Performance can be increased for low and high quality material when the band offsets between *n* and *p*-type material form a robust type-II band alignment that effectively separates electrons and holes even when W is small.

NREL is operated by Midwest Research Institute • Battelle

2008 33rd IEEE Photovoltaic Specialists Conference • San Diego, CA • May 11–16, 2008 • NREL/PO-520-43328